*Article*

# A Fast Motion Parameters Estimation Method Based on Cross-Correlation of Adjacent Echoes for Wideband LFM Radars

**Yixiong Zhang [1],\*, Rujia Hong [1],†, Cheng-Fu Yang [2],\*, Yunjian Zhang [1],†, Zhenmiao Deng [1],†, and Sheng Jin [3],†**

[1] School of Information Science and Engineering, Xiamen University, Xiamen, China; fandsln@163.com (R.H.); zyjdy_2001@sina.com (Y.Z.); dzm_ddb@xmu.edu.cn (Z.D.)

[2] Department of Chemical and Materials Engineering, National University of Kaohsiung, Kaohsiung, Taiwan

[3] Beijing Institute of Tracking and Telecommunications Technology, Beijing, China; jinsheng1101@126.com

\* Correspondence: zyx@xmu.edu.cn (Y.Z.); cfyang@nuk.edu.tw (C.-F.Y.); Tel.:+ 86-592-2965385 (Y.Z.); +00886-7591-9283 (C.-F.Y.).

† These authors contributed equally to this work.

**Abstract:** In wideband radar systems, the performance of motion parameters estimation can significantly affect the performance of object detection and the quality of inverse synthetic aperture radar (ISAR) imaging. Although the traditional motion parameters estimation methods can reduce the range migration (RM) and Doppler frequency migration (DFM) effects in ISAR imaging, the computational complexity is high. In this paper, we propose a new fast non-searching motion parameters estimation method based on cross-correlation of adjacent echoes (CCAE) for wideband LFM signals. A cross-correlation operation is carried out for two adjacent echo signals, then the motion parameters can be calculated by estimating the frequency of the correlation result. The proposed CCAE method can be applied directly to the stretching system, which is commonly adopted in wideband radar systems. Simulational results demonstrate that the new method can achieve better estimation performances, with much lower computational cost, compared with existing methods. The experimental results on real radar data sets are also evaluated to verify the effectiveness and superiority of the proposed method compared to the state-of-the-art existing methods.

**Keywords:** motion parameters estimation, wideband LFM radar, cross-correlation.

## 1. Introduction

The wideband linear frequency modulation (LFM) signal is widely used in modern wideband radar systems. Compared with the narrow-band LFM signal, it can achieve much better quality in inverse synthetic aperture radar (ISAR) imaging, due to the higher range resolution. However, the motions of target often cause range migration (RM) and Doppler frequency migration (DFM) effects in the received signals, which will degrade the imaging quality. Therefore, the object's motion parameters should be estimated and compensated before imaging. Besides, the accuracy of motion parameters estimation also affects the performance of target tracking and identification. Thus, high precision motion parameters estimation is necessary and attracts much more attention in modern wideband radar systems [1–8].

For wideband radars, the estimation methods of motion parameters can be divided into two types: searching methods and non-searching methods. Many of the traditional range alignment methods [8–14] in ISAR imaging are of searching methods, such as spatial domain realignment [8], adaptive joint time-frequency technique [9], minimum entropy method [14]. Spatial domain realignment [8] defines a correlation function between two envelops of echo signals with delays. The amount of envelope shift is determined by searching the delay to obtain the maximum of the correlation function. In [9], the radar echo signal is projected to a set of basis functions, which are constructed with different parameters. A searching procedure is conducted to maximize the projection value, and then the

motion parameters estimated. The minimum entropy method introduces a 1-D entropy function to determine the degree of alignment between radar echoes [14]. As the delay, which minimizes the entropy, is searched with the step determined by the bandwidth of the transmitted signal, the accuracy of the estimated parameters is limited by the delay step. To perform high precision motion parameters estimation, the Radon Fourier transform (RFT) method is proposed for multipulse energy accumulation [5,15,16]. The RFT method is a multidimensional searching method and achieves a good performance of motion parameters estimation because of long coherent integration time. A common drawback of these searching methods is that their computation is highly complex, when they are applied in the wideband radar systems.

In the non-searching methods, the keystone transform (KT) is able to eliminate the RM effect based on long time coherent integration technology [17–19]. But the DFM induced by acceleration cannot be removed by KT. In [20], a non-searching ISAR range alignment method based on minimizing the entropy of the average range profile (ARP) is proposed. An iterative procedure is utilized to estimate the delays of envelops, of which the precision is determined by the range resolution. Meanwhile, an interpolation is employed on the envelops to improve the estimation precision. However, the iterative procedure and the interpolation operation significantly increase the computational complexity. Moreover, the phase information is not used for estimation in [20]. In [21], a novel estimation algorithm of motion parameters is proposed for ISAR imaging, based on KT and the adjacent cross-correlation function (ACCF). Then, a fast non-searching method based on ACCF is proposed for target motion estimation, target detection and ISAR imaging [22–26]. There are two differences between the two methods in [21] and in [22–26]. The first one is that the KT is not utilized in [22–26], and the other one is that the choice of the scaling factors is improved in [26], thus better performance is obtained under low SNR conditions. Compared with the RFT method, the ACCF method [22,23] can achieve similar performance with much lower computational cost. However, it can be applied only to the uncompressed received (UR) signal, whose bandwidth is equal to that of the transmitted wideband LFM signal. In order to reduce the processing bandwidth and the sampling rate of the analog-to-digital converter, the stretching processing is commonly used in most of the wideband LFM radars, and therefore, the ACCF method cannot be applied in these radar systems.

In this paper, a novel and fast estimation method based on cross-correlation of adjacent echoes (CCAE) is proposed. Specifically, the cross-correlation operation is performed on two adjacent echo signals, then the motion parameters are calculated by estimating the frequency of the correlation result. The proposed new method is a non-searching method and can be directly applied to the stretched signals. Since the SNR of the stretched signal is higher than that of the UR signal, better root-mean-square errors (RMSE) performance can be achieved by applying the CCAE method to the stretched signals. When estimating the velocity using two echo signals, the FFT operation is needed only once in the CCAE method. Thus, the computational complexity of the proposed CCAE method is much lower than that of the existing methods. Numerical simulations demonstrate that the proposed CCAE method can be applied in real wideband LFM radars.

The rest of this paper is organized as follows. In Section 2, the model of the stretched signal is presented. In Section 3, the proposed fast non-searching CCAE method is presented first, and then the root mean square error (RMSE) of the proposed CCAE method derived in closed form. In Section 4, the details of the experiments conducted on simulation and real data are presented. Finally, we conclude this paper in Section 5.

## 2. Signal Model

In this paper, the scatterer model of the wideband LFM signal is used. It is assumed that the target is in the far field and the incident wave is a plane wave. The scatterers are located on the line of sight. The range profile of target of wideband radar is illustrated in Figure 1. The parameters that will be frequently used in later derivation are listed in Table 1.
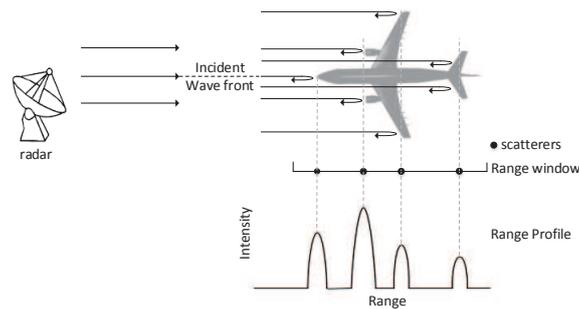
**Figure 1.** Target's range profile of wideband radar

**Table 1.** Notations.

| Notation | Type | Meaning |
|---|---|---|
| $ur$ | Subscript | The received signal is uncompressed. |
| $st$ | Subscript | The signal is stretched. |
| $ac$ | Subscript | The signal is obtained by multiplying a echo signal with the conjugate of another echo signal. |
| $se$ | Subscript | The signal is the multiplication result of the different echo signal from the same scatterers. |
| $cr$ | Subscript | The signal is the multiplication result of the different echo signal from the different scatterers. |
| $s_{tr}(t)$ | Signal | The transmitted signal. |
| $s_{LO}(t)$ | Signal | The local reference signal. |
| $s_{ur}(t,t_m)$ | Signal | The uncompressed received signal. |
| $s_{st}(t,t_m)$ | Signal | The stretched signal. |
| $R_p(t_m)$ | Signal | The distance from radar to the $p$th scatterer. |

The transmitted signal of the wideband LFM radar can be modeled as

$$s_{tr}(t) = \text{rect}\left(\frac{t}{T}\right) e^{j\pi\gamma t^2} e^{j2\pi f_c t}, \tag{1}$$

where $\text{rect}(u) = \begin{cases} 1, |u| \le 1/2 \\ 0, \text{otherwise} \end{cases}$ denotes the rectangle pulse shape, $t$ the fast time, $T$ the pulse width, and $f_c$ the radar center frequency. $\gamma = B/T$ is the chirp rate of the LFM signal, where $B$ is the swept bandwidth of the LFM signal.

The UR signal of the wideband LFM radar can be represented as

$$\begin{aligned}
s_{ur}(t,t_m) &= \sum_{p=0}^{P-1} \text{rect}\left(\frac{t-\tau_p(t_m)}{T}\right) \\
&\quad \times A_p e^{j2\pi f_c(t-\tau_p(t_m))} \\
&\quad \times e^{j\gamma\pi(t-\tau_p(t_m))^2} + \omega_0(t,t_m) \\
&= s_{ur,s}(t,t_m) + \omega_0(t,t_m),
\end{aligned} \tag{2}$$

where $P$ denotes the number of scatterers, $A_p$ the scattering coefficient of the $p$th scatterer, and $\tau_p(t_m)$ the time delay from the radar to the $p$th scatterer. $t_m = mT_{pr}$ is the slow time, where $m$ is the pulse number, and $T_{pr}$ is the pulse repetition interval (PRI). $s_{ur,s}(t,t_m)$ denotes the signal term of $s_{ur}(t,t_m)$, $\omega_0(t,t_m)$ is the Gaussian noise with mean zero and variance $\sigma^2$. The time delay can be expressed as

$$\tau_p(t_m) = \frac{2R_p(t_m)}{c}, \tag{3}$$

where $R_p(t_m)$ is the distance from radar to the $p$th scatterer at slow time $t_m$. Due to the wide bandwidth of the signal, the data size of the uncompressed signal is considerably large, which leads to a high computational complexity. Therefore, in wideband radar systems, stretching operation is often used to reduce the data size.

The local reference signal for stretching operation can be written as

$$s_{LO}(t) = \text{rect}\left(\frac{t}{\hat{T}}\right) e^{-j\left(2\pi f_c t + \pi \gamma t^2\right)}, \tag{4}$$

where $\hat{T}$ is the duration of the reference signal, which is usually slightly larger than the width of the transmitted pulse, so that it covers the received signal. The stretched signal is obtained by multiplication

$$\begin{aligned}
s_{st}(t, t_m) &= s_{ur}(t, t_m) \cdot s_{LO}(t) \\
&= \sum_{p=0}^{P-1} \text{rect}\left(\frac{t - \tau_p(t_m)}{T}\right) A_p e^{-j2\pi\gamma\tau_p(t_m)t} \\
&\quad \times e^{j\pi\gamma\tau_p^2(t_m)} e^{-j2\pi f_c \tau_p(t_m)} + \omega_1(t, t_m) \\
&= s_{st,s}(t, t_m) + \omega_1(t, t_m), \tag{5}
\end{aligned}$$

where $s_{st,s}(t, t_m)$ is the signal term of the $s_{st}(t, t_m)$, $\omega_1(t, t_m) = \omega_0(t, t_m) \cdot s_{LO}(t)$ is the noise. In practical wideband radar systems, the sampling frequency of the stretched signal is much lower than that of the UR signal. Thus, the data size of the stretched signal is much smaller than that of the UR signal. When parameter estimation is performed on the stretched signal, the computational complexity decreases significantly. The proposed motion parameters estimation method can be applied to both UR and stretched signals. In the following section, the idea of "stretching" processing is first illustrated to show the availability of the CCAE method to the UR signal, then the algorithm of the proposed CCAE estimation method is derived using the stretched signal model.

### 3. Estimation of Motion Parameters Based on CCAE Method

*3.1. "Stretching" Idea of Proposed CCAE Method*

In radar systems, when a target is tracked, the range profile of the target varies from pulse to pulse because of the rotational and the translational motions of the target. In this paper, the rotation of target is not taken into consideration. However, within the interval of two adjacent transmitted pulses, the change in motion parameters is generally small. Therefore, the range profiles of two adjacent echo signals are highly correlated [27]. Consequently, the energy of adjacent two echoes can be accumulated. Thus, the motion parameters may be estimated by the correlation result of adjacent echoes.

The idea of the proposed method is shown in Figure 2, where the UR signal is utilized for convenience of illustration. It is already known that stretching operation can transform a wideband echo signal into a narrow-band signal. In the CCAE method, considering one of the two adjacent echo signals (e.g., the echo at slow time $t_m$) as the "local reference" signal, the other one (e.g., the echo at slow time $t_{m+1}$) is "stretched" into a single tone signal. The frequency of the "stretched" signal contains the information of the distance differences between the slow time $t_m$ and $t_{m+1}$. The motion parameters can be estimated according to the distance differences. In the next subsection, the CCAE method is derived mathematically to prove the idea.
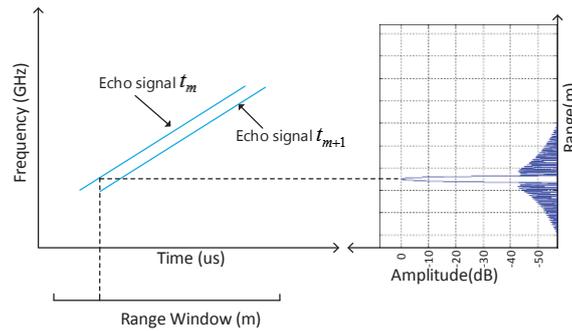
**Figure 2.** The "stretching" idea of the proposed CCAE method

### 3.2. Proposed CCAE Algorithm

At the beginning, we apply the conjugate multiplication to both UR signals and stretched signals. Then it is seen that the conjugate multiplication result of the UR signals is similar to that of the stretched signals. The UR signal at slow time $t_m$ is multiplied with the conjugate of the adjacent UR signal at slow time $t_{m+1}$

$$
\begin{aligned}
s_{ac}^{ur}(t, t_m) &= s_{ur}(t, t_m) \cdot \operatorname{conj}\left(s_{ur}(t, t_{m+1})\right) \\
&= s_{se}(t, t_m) + s_{cr}(t, t_m) + \omega_2^{ur}(t, t_m),
\end{aligned}
\tag{6}
$$

where

$$
\begin{aligned}
s_{se}(t, t_m) = \sum_{p=0}^{P-1} A_p^2 \operatorname{rect}&\left(\frac{t - \tau_p(t_m)}{T}\right) \\
&\times \operatorname{rect}\left(\frac{t - \tau_p(t_{m+1})}{T}\right) \\
&\times e^{j2\pi\gamma\left(\tau_p(t_{m+1}) - \tau_p(t_m)\right)t} \\
&\times e^{j2\pi f_c\left(\tau_p(t_{m+1}) - \tau_p(t_m)\right)} \\
&\times e^{j\pi\gamma\left(\tau_p^2(t_m) - \tau_p^2(t_{m+1})\right)},
\end{aligned}
\tag{7}
$$

$$
\begin{aligned}
s_{cr}(t, t_m) = \sum_{q=0}^{P-1} \sum_{p=0,p\neq q}^{P-1} A_q A_p \operatorname{rect}&\left(\frac{t - \tau_q(t_m)}{T}\right) \\
&\times \operatorname{rect}\left(\frac{t - \tau_p(t_{m+1})}{T}\right) \\
&\times e^{j2\pi\gamma\left(\tau_p(t_{m+1}) - \tau_q(t_m)\right)t} \\
&\times e^{j2\pi f_c\left(\tau_p(t_{m+1}) - \tau_q(t_m)\right)} \\
&\times e^{j\pi\gamma\left(\tau_p^2(t_m) - \tau_q^2(t_{m+1})\right)},
\end{aligned}
\tag{8}
$$

$$
\begin{aligned}
\omega_2^{ur}(t, t_m) = &\,\omega_0(t, t_m)\overline{s_{ur,s}(t, t_{m+1})} \\
&+ \overline{\omega_0(t, t_{m+1})}s_{ur,s}(t, t_m) \\
&+ \omega_0(t, t_m)\overline{\omega_0(t, t_{m+1})},
\end{aligned}
\tag{9}
$$

where the superscript $\bar{x}$ denotes the conjugate of $x$, and the superscript $ur$ indicates that the multiplication is performed on the UR signals. In equation (6), the first term $s_{se}(t, t_m)$ is the product of

adjacent echoes from the same scatterer, the second term $s_{cr}(t, t_m)$ is the product of adjacent echoes from different scatterers, and the third term $\omega_2^{ur}(t, t_m)$ is the noise after conjugate multiplication.

Similarly, when the conjugate multiplication is performed on the stretched signals, we can obtain

$$s_{ac}(t, t_m) = s_{st}(t, t_m) \cdot \text{conj}\left(s_{st}(t, t_{m+1})\right)$$
$$= s_{se}(t, t_m) + s_{cr}(t, t_m) + \omega_2(t, t_m), \tag{10}$$

where

$$\omega_2(t, t_m) = \omega_1(t, t_m)\overline{s_{st,s}(t, t_{m+1})}$$
$$+ \overline{\omega_1(t, t_{m+1})}s_{st,s}(t, t_m)$$
$$+ \omega_1(t, t_m)\overline{\omega_1(t, t_{m+1})} \tag{11}$$

is the noise added to the streched signal after conjugate multiplication. The first two terms of the right hand side of equation (10) are the same in equation (6), where the exponential term $e^{j2\pi\gamma(\tau_p(t_{m+1}) - \tau_p(t_m))t}$ contains the information of the distance difference between the slow time $t_m$ and $t_{m+1}$. The difference lies in that the data rate of the stretched signal is lower than that of the UR signal, and the noise bandwidth is smaller, resulting the SNR of the stretched signal is higher than that of the UR signal. Consequently, the stretched signal is adopted in the following derivation.

In equations (7) and (8), there are two rectangular window functions. The lengths of the two functions are equal, while the positions of them are different. In other words, the nonzero parts of the two window functions do not completely overlap. This will cause loss in signal energy. The length of the non-overlapping part is determined by the target's motion, i.e.,

$$\Delta t_{p,q} = \tau_p(t_{m+1}) - \tau_q(t_m)$$
$$= \frac{2}{c}(R_p(t_{m+1}) - R_q(t_m))$$
$$= \frac{2}{c}\Delta R_{pq}(t_m), \tag{12}$$

where $\Delta R_{pq}(t_m) = R_p(t_{m+1}) - R_q(t_m)$.

In common radar applications, the ratio of the non-overlapping part's length to the length $T$ of the transmitted signal (i.e., $2\Delta R_{pq}(t_m)/cT$) is much less than 1. For example, if $T = 1$ ms and $T_{pr} = 10$ ms, then the length of the target is 50 m and velocity 6000 m/s. Computation of the maximum value of $\Delta R_{pq}(t_m)$ by $\Delta R_{pq}(t_m) = 50 + 6000 \times 0.01 = 110$ m gives the ratio $2\Delta R_{pq}(t_m)/cT \approx 0.073\%$. Thus, the influence of the non-overlapping part can be considered negligible. Then, by substituting equation (3) into equation (10), and applying FFT operation to equation (10) for energy focusing, one gets

$$S_{ac}(f, t_m) = S_{se}(f, t_m) + S_{cr}(f, t_m) + W_2(f, t_m), \tag{13}$$

where $S_{se}(f, t_m)$, $S_{cr}(f, t_m)$, $W_2(f, t_m)$ are the FFT results of $s_{se}(t, t_m)$, $s_{cr}(t, t_m)$ and $\omega_2(t, t_m)$ respectively, i.e.,

$$S_{se}(f, t_m) = \sum_{p=0}^{P-1} A_p^2 \text{sinc}\left[T\left(f - \frac{2\gamma\Delta R_{pp}(t_m)}{c}\right)\right]$$
$$\times e^{j\frac{4\pi}{\lambda_c}\Delta R_{pp}(t_m)} e^{j\frac{4\pi}{c^2}\gamma(R_p^2(t_m) - R_p^2(t_{m+1}))}, \tag{14}$$

$$S_{cr}(f, t_m) = \sum_{q=0}^{P-1} \sum_{p=0, p\neq q}^{P-1} \text{sinc}\left[T\left(f - \frac{2\gamma\Delta R_{pq}(t_m)}{c}\right)\right]$$
$$\times A_q A_p e^{j\frac{4\pi}{\lambda_c}\Delta R_{pq}(t_m)}$$
$$\times e^{j\frac{4\pi}{c^2}\gamma(R_p^2(t_m)-R_q^2(t_{m+1}))}, \tag{15}$$

where $\lambda_c$ is the wavelength corresponding to the center frequency $f_c$. In equations (14) and (15), the exponential terms are constant phase terms, which have no impact on estimating the frequency of the spectrum, i.e., equation (13). For simplicity, the sinc functions are extracted for further discussion in the following sections.

Define

$$S_{si}(f, p, q) = \text{sinc}\left[T\left(f - \frac{2\gamma\Delta R_{pq}(t_m)}{c}\right)\right]. \tag{16}$$

Let it be assumed that the peak position of $S_{si}(f, p, q)$ is $\tilde{f}_{pq}$. When $p = q$, equation (16) is the same as the sinc function in equation (14). Since all scatterers are assumed to locate along the line of sight, the distance difference between $t_m$ and $t_{m+1}$ is the same for every scatterer of the target. Namely, $\Delta R_{pp}(t_m) = \Delta R_{qq}(t_m)$ and $\tilde{f}_{pp} = \tilde{f}_{qq}$ for $p \neq q$. The energy of all scatterers will accumulate on one peak, which can be regarded as the main peak of the spectrum. When $p \neq q$, because of differences in the combinations of $p$ and $q$, the distance difference $\Delta R_{pq}(t_m)$ will bring a number of frequency components $\tilde{f}_{pq}$ ($p \neq q$) into the spectrum. The amplitudes of these spectral lines are much less than that of the main spectral line $\tilde{f}_{pp}$. As seen from equations (12) and (14), the main peak position of the spectrum is determined by the distance difference of target between slow time $t_m$ and $t_{m+1}$. Therefore, the target parameters can be obtained by estimating the frequency of the main peak position. This can be implemented by using the frequency estimation methods, such as FFT and Newton's method [28]. The estimated frequency can be expressed as

$$\hat{f}_m = \frac{2\gamma\Delta R_{pp}(t_m)}{c}$$
$$= \frac{2\gamma(R_p(t_{m+1}) - R_p(t_m))}{c}. \tag{17}$$

Unlike the estimation methods based on coherent integration strategy, the proposed CCAE method is a fast non-searching estimation method, where the estimated parameters can be output in real time. In the following paragraphs, we discuss the algorithm of estimating the velocity and higher order parameters, respectively.

### 3.2.1. Estimation of Velocity

Assuming that only the velocity is taken into consideration, and that the velocities of different scatterers within a target are the same, the motion of the target can be written as

$$R_p(t_m) = R_{0,p} + vt_m, \tag{18}$$

where $R_p(t_m)$ denotes the distance between the $p$th scatterer and the radar at $t_m$ instant, $R_{0,p}$ the initial distance between the $p$th scatterer and the radar, and $v$ the velocity of target. The acceleration of the target $a$ is set to 0. Thus, the estimated frequency $\hat{f}_m$ can be rewritten as

$$\hat{f}_m = \frac{2\gamma(R_p(t_{m+1}) - R_p(t_m))}{c}$$
$$= \frac{2\gamma v T_{pr}}{c}. \tag{19}$$

Consequently, using two echo signals, we can estimate the velocity by the following equation

$$\hat{v} = \frac{c\hat{f}_m}{2\gamma T_{pr}}. \tag{20}$$

### 3.2.2. Estimation of Higher Order Parameters

It is seen from equation (17) that the estimated frequency of the cross-correlation result is determined by the difference in target's distance between the two pulses. To estimate high-order motion parameters, differential operation or curve fitting operation can be applied to the cross-correlation results. For example, a second-order differential operation can be applied to estimate the jerk, with which the acceleration can be obtained using the result of the first-order differential operation. Another approach for simultaneous estimation of velocity, acceleration and other higher order parameters is to employ the curve fitting method, such as the least-square method. But, high-order parameter estimation requires more pulses and consequently the output delay increases. It is worth noting that the objective of the proposed CCAE method is to estimate the motion parameters in real time, i.e., the estimated results should be output with minimum delay. Therefore, for estimation of high-order motion parameters, we mainly focus on acceleration estimation in this paper. Considering the acceleration, equation (18) is rewritten as

$$R_p(t_m) = R_{0,p} + vt_m + \frac{1}{2}at_m^2. \tag{21}$$

Then the estimated frequency $\hat{f}_m$ of equation (17) can be expressed as

$$\hat{f}_m = \frac{2\gamma T_{pr}}{c}(v + at_m + \frac{1}{2}aT_{pr}). \tag{22}$$

It is seen that the estimated frequency is a slow time varied function. The acceleration can be calculated out by $f_m$ and $f_{m+1}$ (i.e., three echo signals are used).

$$\hat{a} = \frac{c}{2\gamma T_{pr}^2}(\hat{f}_{m+1} - \hat{f}_m). \tag{23}$$

Then, the velocity can be obtained with $\hat{f}_0$ at slow time $t_m = mT_{pr}$ $(m = 0)$ and $a$, where $t_m$ $(m = 0)$ can be always set to the time of the first pulse

$$\hat{v} = \frac{c}{2\gamma T_{pr}}f_0 - \frac{1}{2}T_{pr}\hat{a}. \tag{24}$$

### 3.3. Implementation of the Proposed CCAE Method

As described above, the velocity of the target can be estimated by the proposed CCAE method using only two echo signals. To estimate the acceleration or even higher order parameters, three or more echo signals are required. The flow chart of the proposed CCAE method is shown in Figure 3, including the following steps:

1. The first UR or stretched signal is multiplied with the conjugate of the second UR or stretched signal. For acceleration estimation, the second echo signal is also multiplied with the third echo signal.
2. FFT operation is performed on the multiplication results for energy accumulation.
3. Estimate the frequencies of the above FFT results.
4. The acceleration and velocity are calculated using the estimated frequencies according to equations (23) and (24).

Although the ACCF method [22,23] also adopt the conjugate multiplication, it is basically different from the proposed CCAE method. In the ACCF method, first, pulse compression is applied to the two adjacent UR signals by FFT operation and then a conjugate multiplication performed with the pulse compression results. Then, for velocity estimation, the correlation result is transformed into time domain by an IFFT operation. If we only estimate the velocity of the target by using two echo signals, the ACCF method requires FFT (or IFFT) operation three times, while the proposed method only requires once. Besides, the ACCF method can be applied to only the UR signals, while the proposed CCAE method can be applied to both UR and stretched signals.
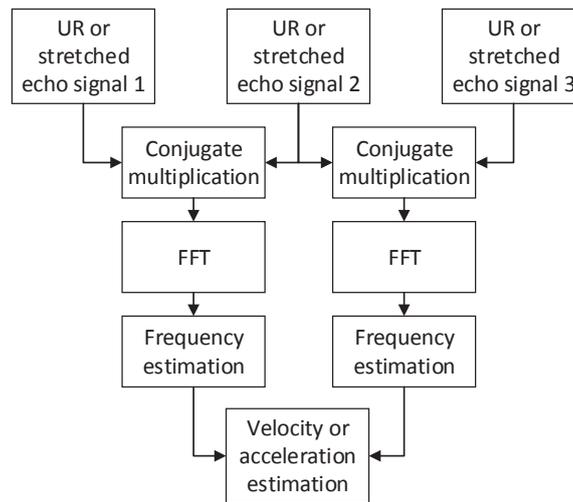


**Figure 3.** The flow chart of proposed CCAE method

*3.4. Performance Analyses*

The SNR of the wideband signal is defined as in [21,29,30]. If the mean of the $\omega_0(t, t_m)$ in equation (2) is zero, and the variance is $\sigma^2$. Then, the SNR of $s_{ur}(t, t_m)$ can be written as $SNR_{ur} = A^2/\sigma^2$, where $A$ is the signal amplitude. Because of the stretching operation and analog-to-digital conversion, the bandwidth of the noise will decrease. If the sampling frequency is $f_s$, then the noise bandwidth of the stretched signal decreases by the ratio $B/f_s$, Consequently, the SNR of the stretched signal, i.e., equation (5), can be written as

$$
\begin{aligned}
SNR_{st} &= \frac{A^2}{\frac{f_s}{B}\sigma^2} \\
&= SNR_{ur}\frac{B}{f_s}.
\end{aligned}
\tag{25}
$$

In equation (10), the first two terms contain the signal and the third one is regarded as the noise term, which is composed of three terms, i.e., $\omega_1(t, t_m)\overline{s_{st,s}(t, t_{m+1})}$, $\overline{\omega_1(t, t_{m+1})}s_{st,s}(t, t_m)$, and $\omega_1(t, t_m)\overline{\omega_1(t, t_{m+1})}$. It is clear that $\omega_1(t, t_m)\overline{s_{st,s}(t, t_{m+1})}$ and $\overline{\omega_1(t, t_{m+1})}s_{st,s}(t, t_m)$ satisfy the Gaussian distribution, and $\omega_1(t, t_m)\overline{\omega_1(t, t_{m+1})}$ satisfy double Gaussian distribution [31], which is approximately regarded as the Gaussian noise in this paper. Therefore, the noise term in equation (10) is approximate to the Gaussian noise. In addition, the means of these three terms are zero, and the variances of them are $A^2\sigma^2 f_s/B$, $A^2\sigma^2 f_s/B$ and $\sigma^4 f_s^2/B^2$, respectively. Hence, the SNR of $s_{ac}(t, t_m)$ is

$$
\begin{aligned}
SNR_{ac} &= \frac{A^4}{\frac{f_s}{B}\left(2A^2\sigma^2 + \frac{f_s}{B}\sigma^4\right)} \\
&= \frac{SNR_{st}}{2 + 1/SNR_{st}}.
\end{aligned}
\tag{26}
$$

The velocity of the target is obtained by estimating the main peak position of the sinc function in equation (13). This procedure can be considered similar to that of frequency estimation of a complex sinusoidal signal $s_{ac}(t, t_m)$. For a complex sinusoidal signal with unknown amplitude, phase and frequency [32], the RMSE of frequency estimation can be expressed as

$$RMSE_f = \sqrt{\frac{6}{4\pi^2 SNR\Delta^2 N(N^2-1)}}, \tag{27}$$

where $\Delta$ is the sampling interval, $N$ the number of samples, and $SNR$ the SNR of the sinusoidal signal [32]. According to the above definition, the RMSE of velocity of the proposed method is

$$\begin{aligned} RMSE_v &= \frac{c}{2\gamma T_{pr}} \sqrt{\frac{6}{4\pi^2 SNR_{ac}\Delta^2 N(N^2-1)}} \\ &= \frac{c}{2\gamma T_{pr}} \sqrt{\frac{6(2Bf_s + f_s^2/SNR_{ur})}{4\pi^2 B^2 SNR_{ur}\Delta^2 N(N^2-1)}}. \end{aligned} \tag{28}$$

When $N$ is large, the equation can be written as

$$\begin{aligned} RMSE_v &\approx \frac{c}{2\gamma T_{pr} T} \sqrt{\frac{6(2Bf_s + f_s^2/SNR_{ur})}{4\pi^2 B^2 SNR_{ur}N}} \\ &= \frac{c}{2BT_{pr}} \sqrt{\frac{6(2Bf_s + f_s^2/SNR_{ur})}{4\pi^2 B^2 SNR_{ur}N}}. \end{aligned} \tag{29}$$

It is seen from equation (29) that the estimation performance is affected by the PRI, the SNR of the UR signal, and the bandwidth $B$. When the acceleration is taken into consideration, the acceleration is obtained by subtracting two i.i.d variables $\hat{f}_m$ and $\hat{f}_{m+1}$ in equation (23). The RMSE of the acceleration can be obtained according to equation (23)

$$\begin{aligned} RMSE_a &= \frac{\sqrt{2}c}{2\gamma T_{pr}^2} \sqrt{\frac{6(2Bf_s + f_s^2/SNR_{ur})}{4\pi^2 (B^2 SNR_{ur})\Delta^2 N(N^2-1)}} \\ &\approx \frac{\sqrt{2}c}{2BT_{pr}^2} \sqrt{\frac{6(2Bf_s + f_s^2/SNR_{ur})}{4\pi^2 B^2 SNR_{ur}N}}, \end{aligned} \tag{30}$$

Similarly, according to equation (24), the velocity is calculated using the subtracted value of the two i.i.d variables $f_0$ and $a$. Thus, the RMSE of the velocity can be expressed as

$$\begin{aligned} RMSE_v &= \frac{3c}{4\gamma T_{pr}} \sqrt{\frac{6(2Bf_s + f_s^2/SNR_{ur})}{4\pi^2 B^2 SNR_{ur}\Delta^2 N(N^2-1)}} \\ &\approx \frac{3c}{4BT_{pr}} \sqrt{\frac{6(2Bf_s + f_s^2/SNR_{ur})}{4\pi^2 B^2 SNR_{ur}N}}. \end{aligned} \tag{31}$$

The energy loss is not considered in the above derived RMSEs. In section 3.2, it is pointed out that the non-overlapping part of the conjugate multiplication result induces loss of signal energy. The loss can be figured out to be small, which has little influences on estimation performance. According to equation (25), conjugate multiplication causes decrease in SNR, consequent to which the performance of the proposed method also suffers. However, since noise bandwidth of the stretched signal is reduced to be much smaller than that of the UR signal, the SNR of the stretched signal is higher than that of the UR signal. Therefore, better estimation performance can be achieved by applying the CCAE method to the stretched signals.

In this paper, the cross-correlation operation is performed on the adjacent two echo signals. Actually, the cross-correlation can be performed on any two echo signals. When the two echo signals are taken with an interval $nT_{pr}$, the "$T_{pr}$" in the equation (29) should be modified as "$nT_{pr}$". As a result, the RMSE will decrease to $RMSE_v/n$. In other words, the performance of the proposed method can be improved through increasing the interval of the echo signals. However, when the interval becomes too large, the correlation between the two echo signals decreases, as a consequence of which the accuracy of parameters estimation decreases. Therefore, for this study, the adjacent two signals are used for parameters estimation.

## 4. Simulations and Real Data Processing

In this section, the proposed CCAE method is first evaluated with different simulation parameters. In section 4.2, the performance of the CCAE method is compared with that of the ACCF method at difference SNRs. Finally, the CCAE method is verified using real radar data.

### 4.1. Evaluation of Proposed CCAE Method

In this subsection, simulations are performed to evaluate the proposed CCAE method. The CPU frequency of the computer is 3.30 GHz, and the memory size is 8 GB. The transmitted signal is an LFM waveform, and additive white Gaussian noise is added to the UR signal. Table 2 lists the detailed simulation parameters. The target is set as a multi-scatterer model containing 10 scatterers, and the length of the target is about 9 m. The velocity is 100 m/s, and the acceleration is set to 0.

**Table 2.** Simulation Parameters of the Evaluation of the Proposed CCAE Method.

| Center frequency (GHz) | Bandwidth (MHz) | Pulse width ($\mu$ s) | ampling frequency (MHz) | PRI (ms) |
|---|---|---|---|---|
| 9 | 200 | 100 | 10 | 5 |

The energy concentration of the proposed CCAE method is investigated at high SNR level, i.e., 30 dB. The spectrum of the cross-correlation result is shown in Figure 4, which shows that the energy of different scatterers is focused on one position. The estimated velocity of the proposed method is 99.9 m/s.
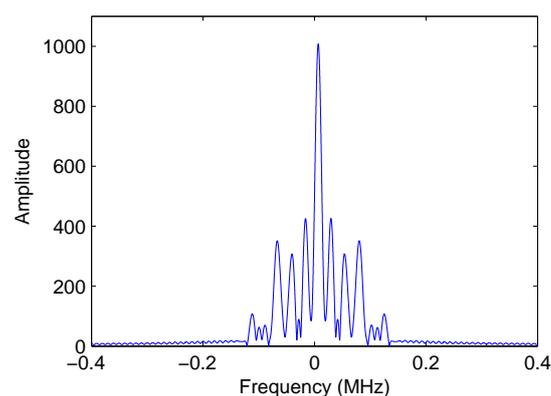


**Figure 4.** The spectrum of the cross-correlation result

Next, we compare the performances of the proposed CCAE method with different bandwidths and PRIs, under different SNR conditions. The SNR varies from -26 dB to 2 dB. Under each SNR, 1000 times of Monte carlo simulations have been carried out. Figure 5 shows the RMSE results. It is observed that when the bandwidth or the PRI increases, the RMSE decreases. To achieve the same RMSE, the test case with $B = 1$ GHz and $T_{pr} = 10$ ms requires the lowest SNR, and hence it has the

best performance. Under the same SNR, the RMSE performance of the case with $B = 1$ GHz, $T_{pr} = 10$ ms is about 3 dB lower than the case with $B = 0.5$ GHz, $T_{pr} = 10$ ms and the case with $B = 1$ GHz and $T_{pr} = 5$ ms. The performance difference is about 6 dB between the case with $B = 1$ GHz, $T_{pr} = 10$ ms and the case with $B = 0.5$ GHz, $T_{pr} = 5$ ms.

**Table 3.** Simulation Parameters of the Comparison with the ACCF Method.

| Center frequency (GHz) | Bandwidth (GHz) | Pulse width ($\mu$ s) | Sampling frequency (MHz) | PRI (ms) |
|:---:|:---:|:---:|:---:|:---:|
| 9 | 1 | 100 | 10 | 10 |
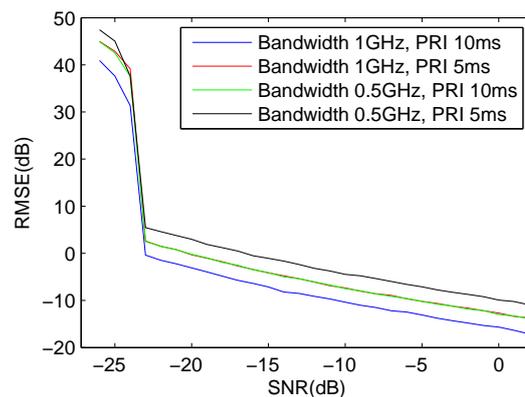


**Figure 5.** The performances of the proposed CCAE method with different parameters

### 4.2. Comparison with ACCF method

In this subsection, we compare the performance of the proposed CCAE method with the ACCF method [22,23] at different SNRs, which varies from -30 dB to 2 dB. 1000 Monte carlo simulations are also carried out for each SNR condition. The other simulation parameters are listed in Table 3. In our simulations, the stretched signals are used in the proposed CCAE method, and the UR signals are used in the ACCF method, which can only be applied to the UR signals.

We first evaluate the performance of the case, in which only velocity is taken into account. The velocity of the target is set to 100 m/s. Two pulse echoes are used for only velocity estimation. In Figure 6, it is seen that the estimated RMSE of the proposed CCAE method outperforms that of the ACCF method. In addition, the estimated RMSE of the proposed CCAE method is close to the theoretical RMSE, which indicates that the error induced by the noise approximation of $\omega_1(t, t_m)\overline{\omega_1(t, t_{m+1})}$ in section 3.4 is small.

We further evaluate the performances of the two methods with a second-order motion model. The velocity of the target is 100 m/s, and the acceleration is 10 m/s$^2$. Three pulses are used for velocity and acceleration estimation, the other parameters being the same as those of the previous experiments. The estimated acceleration results are shown in Figure 7, from which we can see that the RMSE of the CCAE method is much lower than that of the ACCF method. As has already been analyzed in section 3.4, SNR decreases after cross-correlation. To estimate the acceleration, the conjugate multiplication has to be used twice in the ACCF method, but only once in the CCAE method. Therefore, the performance loss is more in the ACCF method than in the CCAE method.

When the acceleration is considered, the velocity estimation results by using CCAE and ACCF methods are compared in Figure 8. It can be seen that the RMSE of the ACCF method is also larger than the proposed method. To estimate the velocity, the estimated acceleration should be used to eliminate its influence. Thus, the performance of the velocity estimation is related to the performance of the acceleration estimation. As the performance of estimated acceleration is worse, the performance

of velocity estimation of the ACCF method also becomes worse. In addition, for the proposed method, the RMSEs of the estimated acceleration and velocity are both close to the theoretical RMSEs, which proves the effectiveness of the proposed method. From a comparison of Figure 6 and Figure 8, for the proposed CCAE method, it can be seen that the RMSE of the estimated velocity with acceleration is a bit higher than that without acceleration. This is because the velocity is calculated by subtracting two i.i.d variables. This can be confirmed by comparing equation (29) and (31).
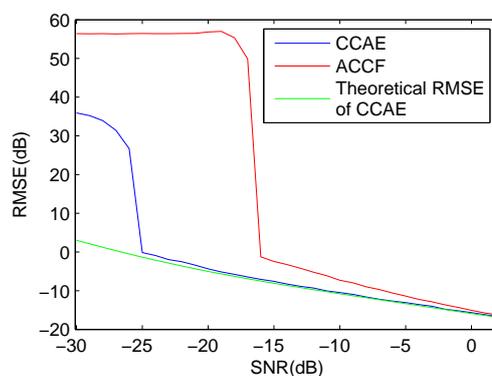


**Figure 6.** Comparison of RMSE results of the velocity estimation by using CCAE and ACCF methods (without acceleration)
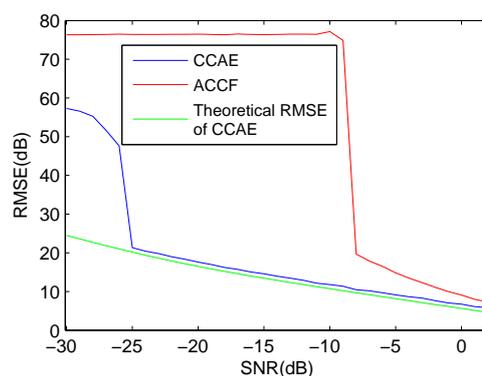


**Figure 7.** Comparison of RMSE results of the acceleration estimation by using CCAE and ACCF methods (with acceleration)
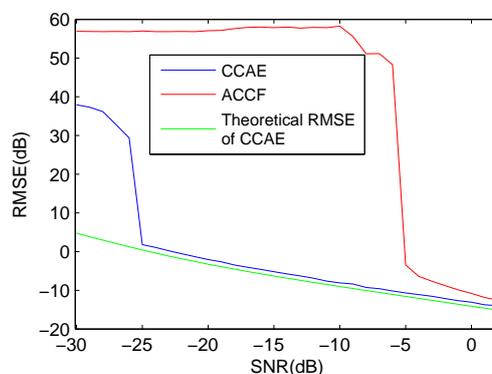


**Figure 8.** Comparison of RMSE results of the velocity estimation by using CCAE and ACCF methods (with acceleration)

The total time costs of the 1000 Monte carlo simulations for all the SNR cases are listed in Table 4. It is seen that the time cost of the proposed CCAE method is much smaller than that of the ACCF method. The reason is two-fold: first, the data size of the UR signal is larger than the stretched signal; second, the number of FFT operation required by the ACCF method is more than that of the CCAE method.

**Table 4.** Comparison of the Time Cost between CCAE and ACCF

| Time cost (s) | CCAE | ACCF |
|---|---|---|
| Estimation without acceleration | 81.6 | 5282.1 |
| Estimation with acceleration | 156.5 | 10175.3 |

Simulation environment: CPU frequency 3.30 GHz, memory 8 GB.

### 4.3. Verification with Real Data

Two sets of real data, obtained from the wideband LFM radar systems are applied for the verification of the proposed method. The parameters of the two data sets are shown in Table 5. The targets are satellites. Figure 9(a) and Figure 10(a) show the estimated velocities in comparison with the real velocities of the targets. The errors between the estimated velocities and the real velocities of the targets are shown in Figure 9(b) and Figure 10(b). It is seen that the estimated results are consistent with the real velocities for both the data sets. The RMSE of the estimated velocity is 0.0561 m/s in the first data set and 0.2842 m/s in the second data set.

**Table 5.** Parameters of Radars.

| Parameters | Radar 1 | Radar 2 |
|---|---|---|
| Center Frequency (GHz) | 9 | 3.2 |
| Bandwidth (MHz) | 2000 | 300 |
| Sampling Frequency (MHz) | 10 | 10 |
| Pulse Width ($\mu$s) | 400 | 200 |
| PRI (ms) | 40 | 100 |
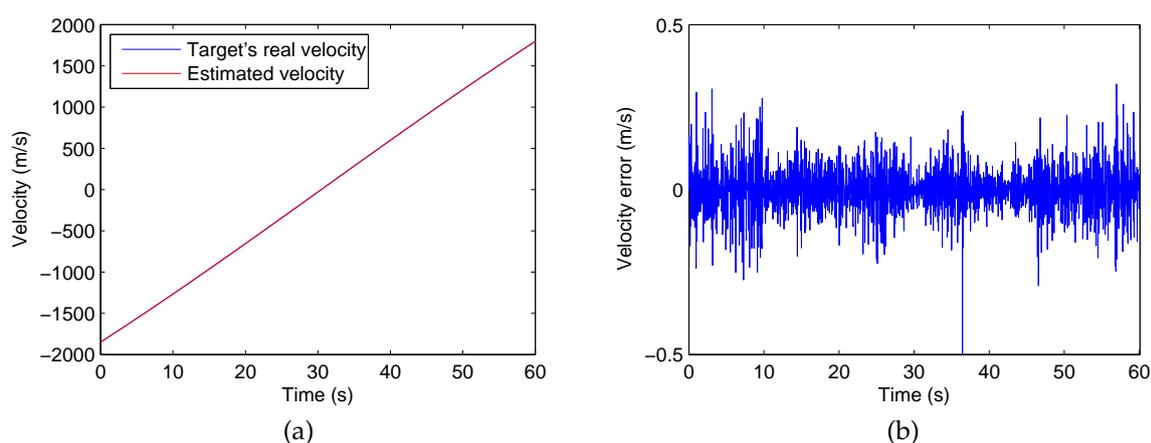


**Figure 9.** Estimation results of data set 1. (**a**) The estimated velocity and the target's real velocity. (Due to the high speed of the target and the high precision of the estimated velocity, the two lines overlap). (**b**) The error between the estimated velocity and the target's real velocity.

(a)                                                             (b)
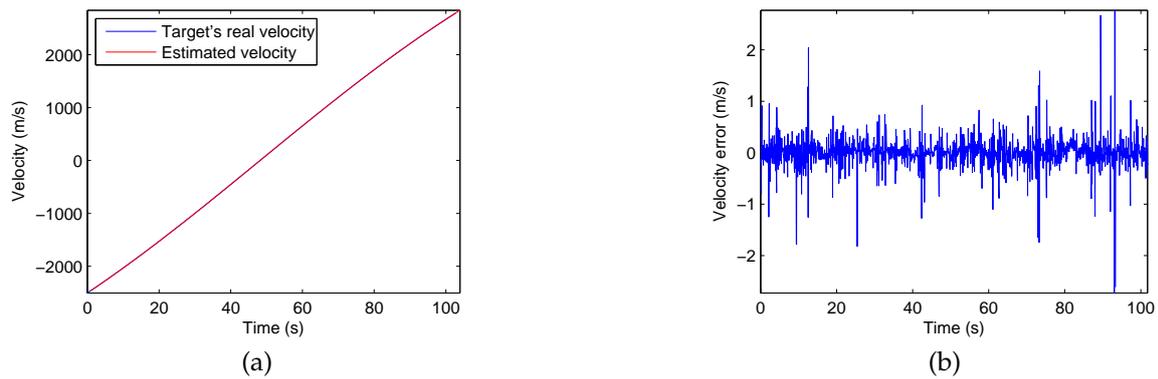
**Figure 10.** Estimation results of data set 2. (**a**) The estimated velocity and real velocity of the target. (Due to the high speed of the target and the high precision of the estimated velocity, the two lines overlap). (**b**) The error between the estimated velocity and the target's real velocity.

Finally, the proposed CCAE method is applied to range alignment in ISAR imaging procedure, with a civil aircraft as the target. Figure 11(a) shows the range profile with RM, caused mainly by the target's velocity. Thus, it can be corrected by compensating the estimated velocities in the range profile. The result of range alignment, obtained by using the proposed method, is shown in Figure 11(b), from which it can be seen that the RM effect is eliminated, resulting in a focused ISAR image (Figure 12). These results with real data demonstrate that the proposed method is effective in practical radar systems.



(a)                                                             (b)
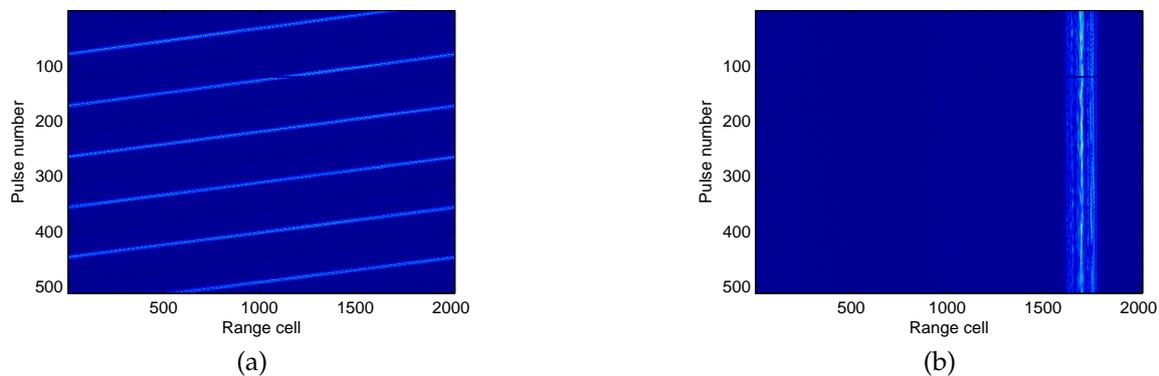
**Figure 11.** The range profile of the target. (**a**) The range profile with RM effect. (**a**) The range profile after range alignment by the proposed CCAE method.
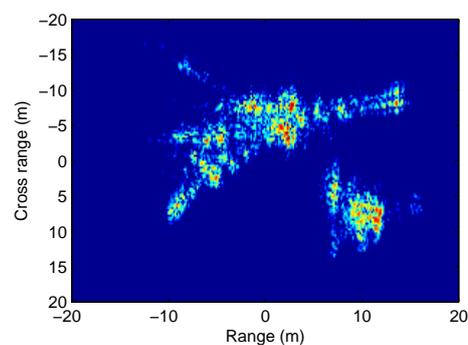


**Figure 12.** The result of ISAR imaging after range alignment

## 5. Conclusion

In this paper, a new fast motion parameters estimation method based on CCAE for wideband LFM radars is presented. First, the conjugate multiplication is performed on the adjacent two signals. Then the velocity is obtained by estimating the frequency of the signal, i.e., the correlation result. The acceleration can be estimated by using three echo signals. The proposed CCAE method can be applied to the UR signals or the stretched signals. When estimating the velocity using two echo signals, the FFT operation is required only once in the proposed method, and the estimated parameters can be output in real time. Simulation results show that the new method provides better RMSE performances than the state-of-the-art existing method for both velocity and acceleration estimation, with much less computational cost. Besides, the RMSEs of the simulation data are close to the theoretical RMSEs of the proposed method. Real radar data sets are also evaluated to verify the effectiveness of the proposed method. The proposed fast estimation method of motion parameters can be applied to range alignment in ISAR imaging.

**Author Contributions:** Yi-xiong Zhang, Zhen-miao Deng and Cheng-Fu Yang conceived and designed the experiments; Ru-jia Hong performed the experiments; Yun-jian Zhang analyzed the data; Cheng-Fu Yang and Sheng Jin contributed reagents/materials/analysis tools; Yi-xiong Zhang and Ru-jia Hong wrote the paper; Yi-xiong Zhang, Zhen-miao Deng and Cheng-Fu Yang modified the paper.

**Conflicts of Interest:** The authors declare that the grant, scholarship and/or funding mentioned in the Acknowledgments section do not lead to any conflict of interest. Additionally, the authors declare that there is no conflict of interest regarding the publication of this manuscript.

## References

1. Skolnik, M.I. Introduction to radar. *Radar Handbook* **1962**, *2*.
2. Werness, S.A.; Carrara, W.G.; Joyce, L.; Franczak, D.B. Moving target imaging algorithm for SAR data. *IEEE Transactions on Aerospace and Electronic Systems* **1990**, *26*, 57–67.
3. Chen, V.C.; Qian, S. Joint time-frequency transform for radar range-Doppler imaging. *IEEE Transactions on Aerospace and Electronic Systems* **1998**, *34*, 486–499.
4. Berizzi, F.; Mese, E.D.; Diani, M.; Martorella, M. High-resolution ISAR imaging of maneuvering targets by means of the range instantaneous Doppler technique: modeling and performance analysis. *IEEE Transactions on Image Processing* **2001**, *10*, 1880–1890.
5. Yu, J.; Xu, J.; Peng, Y.N.; Xia, X.G. Radon-Fourier transform for radar target detection III: optimality and fast implementations. *IEEE Transactions on Aerospace and Electronic Systems* **2012**, *48*, 991–1004.
6. Suo, P.C.; Tao, S.; Tao, R.; Nan, Z. Detection of high-speed and accelerated target based on the linear frequency modulation radar. *IET Radar, Sonar & Navigation* **2014**, *8*, 37–47.
7. Peng, S.B.; Xu, J.; Peng, Y.N.; Xiang, J.B. Parametric inverse synthetic aperture radar manoeuvring target motion compensation based on particle swarm optimiser. *IET radar, sonar & navigation* **2011**, *5*, 305–314.
8. Chen, C.C.; Andrews, H.C. Target-motion-induced radar imaging. *IEEE Transactions on Aerospace and Electronic Systems* **1980**, *16*, 2–14.
9. Wang, Y.; Ling, H.; Chen, V.C. ISAR motion compensation via adaptive joint time-frequency technique. *IEEE Transactions on Aerospace and Electronic Systems* **1998**, *34*, 670–677.
10. Wang, J.; Kasilingam, D. Global range alignment for ISAR. *IEEE Transactions on Aerospace and Electronic Systems* **2003**, *39*, 351–357.
11. Li, J.; Wu, R.; Chen, V.C. Robust autofocus algorithm for ISAR imaging of moving targets. *IEEE Transactions on Aerospace and Electronic Systems* **2001**, *37*, 1056–1069.
12. Wu, H.; Grenier, D.; Delisle, G.Y.; Fang, D.G. Translational motion compensation in ISAR image processing. *IEEE Transactions on Image Processing* **1995**, *4*, 1561–1571.
13. Xing, M.; Wu, R.; Lan, J.; Bao, Z. Migration through resolution cell compensation in ISAR imaging. *IEEE Geoscience and Remote Sensing Letters* **2004**, *1*, 141–144.

14.   Xi, L.; Guosui, L.; Ni, J. Autofocusing of ISAR images based on entropy minimization. *IEEE Transactions on Aerospace and Electronic Systems* **1999**, *35*, 1240–1252.

15.   Xu, J.; Yu, J.; Peng, Y.N.; Xia, X.G. Radon-Fourier transform for radar target detection, I: generalized Doppler filter bank. *IEEE Transactions on Aerospace and Electronic Systems* **2011**, *47*, 1186–1202.

16.   Xu, J.; Xia, X.G.; Peng, S.B.; Yu, J.; Peng, Y.N.; Qian, L.C. Radar maneuvering target motion estimation based on generalized Radon-Fourier transform. *IEEE Transactions on Signal Processing* **2012**, *60*, 6190–6201.

17.   Perry, R.; Dipietro, R.; Fante, R. SAR imaging of moving targets. *IEEE Transactions on Aerospace and Electronic Systems* **1999**, *35*, 188–200.

18.   Zhu, D.; Li, Y.; Zhu, Z. A keystone transform without interpolation for SAR ground moving-target imaging. *IEEE Geoscience and Remote Sensing Letters* **2007**, *4*, 18–22.

19.   Li, G.; Xia, X.G.; Peng, Y.N. Doppler keystone transform: an approach suitable for parallel implementation of SAR moving target imaging. *IEEE Geoscience and Remote Sensing Letters* **2008**, *5*, 573–577.

20.   Zhu, D.; Wang, L.; Yu, Y.; Tao, Q.; Zhu, Z. Robust ISAR range alignment via minimizing the entropy of the average range profile. *IEEE Geoscience and Remote Sensing Letters* **2009**, *6*, 204–208.

21.   Li, Y.; Xing, M.; Su, J.; Quan, Y.; Bao, Z. A new algorithm of ISAR imaging for maneuvering targets with low SNR. *IEEE Transactions on Aerospace and Electronic Systems* **2013**, *49*, 543–557.

22.   Li, X.; Cui, G.; Yi, W.; Kong, L. A fast maneuvering target motion parameters estimation algorithm based on ACCF. *IEEE Signal Processing Letters* **2015**, *22*, 270–274.

23.   Li, X.; Cui, G.; Kong, L.; Yi, W. Fast Non-Searching Method for Maneuvering Target Detection and Motion Parameters Estimation. *IEEE Transactions on Signal Processing* **2016**, *64*, 2232–2244.

24.   Lv, X.; Bi, G.; Wan, C.; Xing, M. Lv's distribution: principle, implementation, properties, and performance. *IEEE Transactions on Signal Processing* **2011**, *59*, 3576–3591.

25.   Luo, S.; Bi, G.; Lv, X.; Hu, F. Performance analysis on Lv distribution and its applications. *Digital Signal Processing* **2013**, *23*, 797–807.

26.   Li, X.; Kong, L.; Cui, G.; Yi, W.; Yang, Y. ISAR imaging of maneuvering target with complex motions based on ACCF–LVD. *Digital Signal Processing* **2015**, *46*, 191–200.

27.   Shui, P.L.; Xu, S.W.; Liu, H.W. Range-spread target detection using consecutive HRRPs. *IEEE Transactions on Aerospace and Electronic Systems* **2011**, *47*, 647–665.

28.   Abatzoglou, T.J. A fast maximum likelihood algorithm for frequency estimation of a sinusoid based on Newton's method. *IEEE Transactions on Acoustics, Speech and Signal Processing* **1985**, *33*, 77–89.

29.   Xia, X.G. A quantitative analysis of SNR in the short-time Fourier transform domain for multicomponent signals. *IEEE Transactions on Signal Processing* **1998**, *46*, 200–203.

30.   Xia, X.G.; Chen, V.C. A quantitative SNR analysis for the pseudo Wigner-Ville distribution. *IEEE Transactions on Signal Processing* **1999**, *47*, 2891–2894.

31.   O'Donoughue, N.; Moura, J.M.F. On the Product of Independent Complex Gaussians. *IEEE Transactions on Signal Processing* **2012**, *60*, 1050–1063.

32.   Rife, D.; Boorstyn, R. Single tone parameter estimation from discrete-time observations. *IEEE Transactions on Information Theory* **1974**, *20*, 591–598.